This is the **accepted version** of the journal article:

Su, Lijuan; Muñoz Enano, Jonathan; Vélez Rasero, Paris; [et al.]. «Highly sensitive phase variation sensors based on step-impedance coplanar waveguide (CPW) transmission lines». IEEE Sensors Journal, Vol. 21, issue 3 (Feb. 2021), p. 2864-2872. DOI 10.1109/JSEN.2020.3023848

This version is available at https://ddd.uab.cat/record/283332

under the terms of the IN COPYRIGHT license

Highly Sensitive Phase Variation Sensors Based on Step-Impedance Coplanar Waveguide (CPW) Transmission Lines

Lijuan Su, Jonathan Muñoz-Enano, Paris Vélez, *Member IEEE*, Pau Casacuberta, Marta Gil, and Ferran Martín, *Fellow, IEEE*

***Abstract*—Reflective-mode step-impedance transmission line based sensors for dielectric characterization of solids or liquids have been recently proposed. In this paper, in order to further increase the sensitivity, the sensor is implemented in coplanar waveguide (CPW technology), and this constitutes the main novelty of this work. The sensor thus consists of a high-impedance 90º (or low-impedance 180º) open-ended sensing line cascaded to a low-impedance 90º (or high-impedance 90º) line. The output variable is the phase of the reflection coefficient, which depends on the dielectric constant of the material under test (MUT), the input variable. Placing a MUT on top of the sensing line causes a variation in the effective dielectric constant of the line, thereby modifying the phase of such line. This in turn produces a multiplicative effect on the phase of the reflection coefficient, by virtue of the step-impedance discontinuity. The main advantage of the CPW-based sensor, over other similar sensors based on microstrip technology, is the stronger dependence of the phase velocity of the sensing line with the dielectric constant of the MUT, resulting in sensitivities as high as –45.48º in one of the designed sensors. The sensor is useful for dielectric characterization of solids and liquids, and for the measurement of variables related to changes in the dielectric constant of the MUT (defect detection, material composition, etc.).**

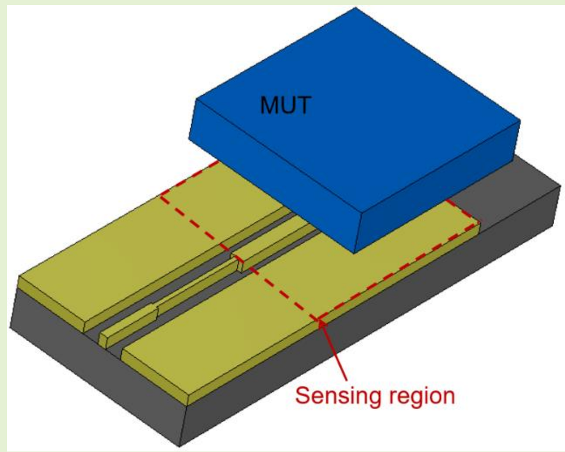

***Index Terms*— CPW technology, dielectric characterization, microwave sensors, phase-variation sensors, reflective-mode sensors.**

I. INTRODUCTION

PLANAR microwave sensors have been a subject of increasing investigation in recent years, especially for the characterization of solids or liquids. There are several reasons that justify such interest, among them, their low-cost, their compatibility with fully planar fabrication technologies (including also additive, i.e., printing, processes), their robustness against harsh conditions (at least as compared to optical sensors), or the possibility to combine microwave technologies with other technologies of interest for sensing (e.g., microfluidics, lab-on-a-chip, organ-on-a-chip, 3D-printing, conformal sensors, organic sensors, etc.). Additionally, microwaves are very sensitive to the properties of the materials to which they interact, and therefore microwave sensors are very interesting for material characterization. To conclude the list of advantageous aspects, let us mention that a key aspect of microwave sensors concerns the low-cost of the associated circuitry needed for post-processing or for communication purposes.

There are many different approaches for the implementation of planar microwave sensors, and several classification schemes, based on various criteria, can be considered. For instance, planar microwave sensors can be categorized according to the range of working frequencies, to the application, or to the working principle, among others, the latter one being typically the most convenient for comparison

This work was supported by MINECO-Spain (project TEC2016-75650-R), by *Generalitat de Catalunya* (project 2017SGR-1159), by *Institució Catalana de Recerca i Estudis Avançats* (who awarded Ferran Martín), and by FEDER funds. J. Muñoz-Enano acknowledges Secreteraria d'Universitats i Recerca (Gen. Cat.) and European Social Fund for the FI grant. Paris Vélez acknowledges the Juan de la Cierva Program for supporting him through Project IJCI-2017-31339. M. Gil acknowledges the Universidad Politécnica de Madrid Young Researchers Support Program (VJIDOCUPM18MGB) for its support.

L. Su, J. Muñoz-Enano, P. Vélez, P. Casacuberta and F. Martín are with GEMMA/CIMITEC, Departament d'Enginyeria Electrònica, Universitat Autònoma de Barcelona, 08193 Bellaterra, Spain. E-mail: Ferran.Martin@uab.es.
M. Gil is with Departamento Ingeniería Audiovisual y Comunicaciones, Universidad Politécnica de Madrid, 28031 Madrid, Spain.

XXXX-XXXX © XXXX IEEE. Personal use is permitted, but republication/redistribution requires IEEE permission.
See http://www.ieee.org/publications_standards/publications/rights/index.html for more information.

purposes (i.e., comparing sensors based on different principles is not easy). Thus, according to the working principle, planar microwave sensors can be essentially divided into frequency-variation sensors [1]-[16], phase-variation sensors [17]-[21], frequency-splitting sensors [22]-[28], coupling-modulation sensors [29]-[39], and differential-mode sensors [17],[18],[40]-[49]. It should be mentioned, however, that, sometimes, it is difficult to classify a sensor within a specific group (e.g., differential-mode phase-variation sensors have been reported [17],[18]).

In most reported planar microwave sensors, wideband signals are typically required for sensing (note that this is a requirement in frequency-variation and frequency-splitting sensors). This increases the cost of the associated electronics. Hence, there is an increasing interest for the implementation of microwave sensors based on single-frequency measurements. In this paper we propose a phase-variation sensor operating at a single frequency, aimed to the measurement of the dielectric constant of solid materials (i.e., the so-called material under test –MUT). The sensor is a one-port structure operating in reflection (other reflective-mode sensors have been recently reported [21],[50],[51]), and the output variable is the phase of the reflection coefficient. The sensor is based on a step-impedance transmission line, where the sensing region is constituted by the open-ended transmission line section, either a high-impedance 90º line, or a low-impedance 180º line, as it will be shown. Indeed, such reflective-mode step-impedance phase-variation sensors were already introduced in [21] by the authors, where implementation in microstrip technology was considered. In this paper, the two designed prototype sensors have been fabricated in coplanar waveguide (CPW) technology, as far as CPW transmission lines exhibit significantly stronger dependence of their phase on the dielectric constant of the MUT (the input variable). By this means, sensor sensitivity, the key figure of merit, can be further enhanced. This is the reason for choosing the CPW configuration, and constitutes the main novelty of the present paper.

The paper is organized as follows: the working principle of the sensor, including a comparative analysis (with the microstrip counterpart) relative to the potential for sensitivity enhancement, is reported in Section II. Section III is focused on the design of two prototype sensors and validation at simulation level. Details of sensor fabrication, and experimental validation are carried out in Section IV, where the phase of the reflection coefficient corresponding to several MUTs is reported. A comparison with other similar sensors is carried out in Section V. Finally, Section VI concludes the work.

II. Working Principle and Sensitivity Enhancement

The typical topology of the proposed sensors is depicted in Fig. 1. The sensor consists of an open-ended sensing line, with electrical length ϕ_s at the operating frequency, f_0, and characteristic impedance Z_s, cascaded to a step-impedance transmission line, designated as design line [21]. By loading the sensing line with a MUT, the effective dielectric constant of the sensing line is altered, thereby producing a variation in the phase and characteristic impedance of the sensing line. This, in turn, modifies the phase of the reflection coefficient, which can be used as output variable for sensing the dielectric constant of the MUT.

The step-impedance line is constituted by several sections with alternating high and low impedance. The sensitivity is proportional to the product of the impedance contrast of the different sections, provided the electrical length and characteristic impedance of the sensing line and transmission line sections of the step-impedance design line are adequately chosen [21]. Thus, the sensing line can be either a high-impedance 90º line or a low-impedance 180º line. In the former case, the transmission line section of the step-impedance design line adjacent to the sensing line must be a low impedance 90º line, and the subsequent line sections must exhibit high and low impedance alternating, and their electrical length must be 90º. For the low-impedance 180º sensing line, the step-impedance design line must be constituted by 90º sections, also with alternating high and low impedance, but in this case, the section adjacent to the sensing line must exhibit high impedance. With the above-indicated design criteria, the sensitivity for small perturbations is optimized, as it was demonstrated in [21].

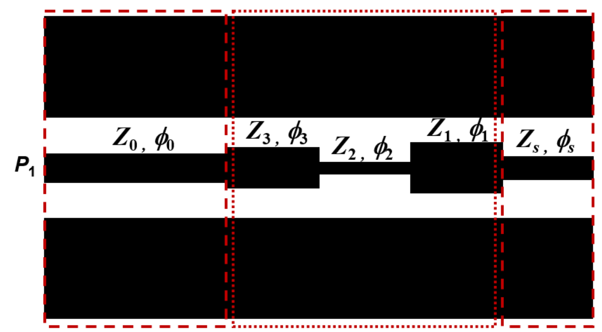

Fig. 1. Typical topology of the proposed reflective-mode step-impedance phase variation sensor. The design line in this illustrative example is a step-impedance line with N = 3 quarter-wavelength sections, and the sensing line is a high-impedance 90º line.

The sensor sensitivity, defined as the variation of the phase of the reflection coefficient, ϕ_ρ, with the dielectric constant of the material under test, ε_{MUT}, can be expressed as

$$S = \frac{d\phi_\rho}{d\varepsilon_{MUT}} = \frac{d\phi_\rho}{d\phi_s}\frac{d\phi_s}{d\varepsilon_{MUT}} + \frac{d\phi_\rho}{dZ_s}\frac{dZ_s}{d\varepsilon_{MUT}} \tag{1}$$

Although a variation in ε_{MUT} modifies Z_s, as the last term of the right-hand side member in (1) indicates, the derivative $d\phi_\rho/dZ_s$ is null for the phase conditions that optimize the sensitivity (indicated above) and can be neglected [21]. The first derivative of the first term of the right-hand side member in (1), designated as $S_{\phi_s} = d\phi_\rho/d\phi_s$, is controlled by the impedance contrasts of the different line sections, as mentioned before. The higher the number of line sections, the larger the value of S_{ϕ_s}. The derivative $d\phi_s/d\varepsilon_{MUT}$ depends on the specific line type, substrate material and, in general, on the transverse geometry of the sensing line. To optimize the overall sensitivity by considering a small number of sections and moderate impedance contrasts (this reduces sensor size and eases its implementation), it is convenient to enhance such term as much as possible. In [21], the designed sensors were fabricated in microstrip technology. In this paper, the designed sensors are implemented in CPW technology, since the phase of these lines is significantly more sensitive to the dielectric constant of the surrounding medium (i.e., the MUT). Since the main purpose of the paper is to demonstrate the sensitivity enhancement of CPW over microstrip sensing lines, the prototype sensors in this work will be designed by considering only a single stage step-impedance design line (corresponding to the schematic of Fig. 1, but considering $N = 1$).

Let us now focus the attention on the term $d\phi_s/d\varepsilon_{MUT}$, given by

$$\frac{d\phi_s}{d\varepsilon_{MUT}} = \frac{d\phi_s}{d\varepsilon_{eff}}\frac{d\varepsilon_{eff}}{d\varepsilon_{MUT}} \tag{2}$$

The first term of the right-hand side member in (2) can be simply inferred by expressing the phase of the sensing line in terms of the effective dielectric constant of the line, ε_{eff}, i.e.,

$$\phi_s = \frac{\omega_0 l_s}{c}\sqrt{\varepsilon_{eff}} \tag{3}$$

where l_s is the length of the sensing line, $\omega_0 = 2\pi f_0$ is the angular frequency, and c is the speed of light in vacuum. Concerning the second term, the effective dielectric constant of a CPW transmission line depends on its transverse geometry, substrate material, and dielectric constant and thickness of the MUT. Analytical expressions by considering air as MUT can be found in the available literature. Such expressions are complex, and further complexity results by considering a MUT different than air, with a finite width. Therefore, in the present analysis, for the sake of simplicity, we will consider that the thickness of the substrate and MUT are semi-infinite. In practice, this means that the substrate and the MUT (necessarily finite) extend beyond the regions of influence of the electromagnetic field generated by the line. Such hypothesis is plausible in CPWs with slot widths smaller than the substrate and MUT thickness. Under these simplifying assumptions, the effective dielectric constant of the CPW transmission line can be approximated by

$$\varepsilon_{eff} = \frac{\varepsilon_r + \varepsilon_{MUT}}{2} \tag{4}$$

where ε_r is the dielectric constant of the substrate. Note that (4) is easily inferred by considering that the CPW line capacitance is merely given by the parallel connection of the substrate and MUT capacitance (reasonable under the considered simplifying assumptions, and by considering a CPW metal layer of negligible thickness).

Using (3) and (4), (2) is found to be

$$\frac{d\phi_s}{d\varepsilon_{MUT}} = \frac{\omega_0 l_s}{2\sqrt{2}c}\frac{1}{\sqrt{\varepsilon_r + \varepsilon_{MUT}}} \tag{5}$$

As expected, the sensitivity increases with frequency and with the length of the sensing line [18]. It also depends on the dielectric constant of the substrate (a small value of ε_r is convenient for sensitivity improvement). However, it does not depend on the transverse geometry of the line (provided the substrate and MUT are thick enough, as specified before). By comparing (5) with the corresponding expression for microstrip technology, reproduced below [21],

$$\frac{d\phi_s}{d\varepsilon_{MUT}} = \frac{\omega_0 l_s}{2\sqrt{2}c}\frac{1}{\sqrt{\varepsilon_r\frac{1+F}{(1-F)^2} + \varepsilon_{MUT}\frac{1}{1-F}}} \tag{6}$$

it can be concluded that the sensitivity is better by considering a CPW sensing line. In (6), F is a geometry factor that depends on the substrate thickness, h, and width of the microstrip sensing line, W_s, according to [52]

$$F = \left(1 + 12\frac{h}{W_s}\right)^{-1/2} \tag{7}$$

The previous expression is valid as far as $W_s > h$ and $t << h$, where t is the thickness of the metallic layer. Note that F is a positive number smaller than 1, consequently, the weighting factors of ε_r and ε_{MUT} in the square root of (6) are larger than 1. Therefore, it is clear that, for the same value of length and frequency, the sensitivity of the phase of the sensing line with the dielectric constant of the MUT is larger in CPW transmission lines. It should also be mentioned that although a small value of ε_r favors sensitivity (as indicated before), this aspect is not critical for sensitivity optimization. The fundamental aspect for sensitivity enhancement is to implement a stepped-impedance structure with high impedance contrast and the adequate electrical lengths of both the sensing line and the line section cascaded to it, as it will be later shown.

To demonstrate the previous conclusion, we have carried out full-wave electromagnetic simulations by considering a CPW and a microstrip open-ended sensing line loaded with a semi-infinite MUT of varying dielectric constant. Let us consider in both cases that the characteristic impedance of the bare line is $Z_s = 35\ \Omega$, and that the parameters of the substrate are those of the *Rogers RO3010* substrate, with thickness h = 1.27 mm and dielectric constant $\varepsilon_r = 10.2$. Losses are excluded in these simulations for coherence with the previous analysis. Nevertheless, this is justified since low-loss microwave substrates (for example, the *Rogers RO3010* family), typically used in microwave sensors, exhibit very small loss tangents. With these substrate parameters, and characteristic impedance, the width of the microstrip line is W_s = 2.12 mm, whereas the line and slot widths for the CPW transmission line are W_s = 2.26 mm and S_s = 0.27 mm, respectively. The resulting geometrical parameters satisfy the aforementioned simplifying assumptions (for that purpose, the characteristic impedance of the lines has been deliberately set to a small value). Concerning the length of the lines, it has been set to the necessary value to implement 180º sensing lines, as this electrical length maximizes the sensitivity for low-impedance sensing lines, as reported in [21] (note that the simulated structures do not include the step-impedance design line, since in this simulation analysis we are merely interested on the effects of ε_{MUT} variation on the phase of the sensing line). Thus, for the CPW and microstrip line such lengths are l_s = 32.25 mm and l_s = 26.17 mm, respectively (the considered operating frequency is f_0 = 2 GHz).

Figure 2 depicts the dependence of the phase of the lines with the dielectric constant of the MUT for both lines. This phase has been indirectly inferred from the phase of the simulated reflection coefficient by considering a reference impedance identical to the characteristic impedance of the line loaded with the MUT (the impedance of the line has been inferred by using the *CST Microwave Studio* commercial software). Under these conditions, the phase of the reflection coefficient, the simulated parameter, is twice the phase of the line [21]. Note that the variation is stronger for the CPW transmission line, as predicted by the analysis. Therefore, it can be concluded that the overall sensitivity, magnified by the presence of the step-impedance design line, will be better by implementing the sensor in CPW technology. We have represented in the same figure the sensitivities, inferred by simply deriving the simulated data points. Such sensitivities are in good agreement with the analytical curves given by (5) and (6), also represented. Such good agreement with the simulated data points out the validity of the analysis and the considered approximations.

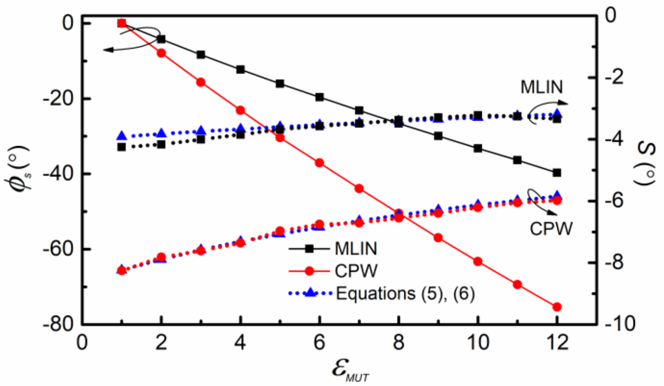

Fig. 2. Dependence of the phase of the open-ended 180º and 35 Ω CPW and microstrip (MLIN) sensing lines with the dielectric constant of the semi-infinite MUT. The sensitivities are also included. The curves with triangular symbols correspond to the analytical (5) and (6). The electromagnetic simulations have been carried out by means of the *CST Microwave Studio* commercial software.

III. Sensor Design and Simulations

In this section, two prototype reflective-mode phase-variation sensors based on a step-impedance configuration and implemented in CPW technology are designed. In one sensor (designated as sensor A), the sensing line is an open-ended 180º line with low characteristic impedance, i.e., Z_s = 35 Ω. The operating frequency is set to f_0 = 2 GHz. In this work, where the main aim is to demonstrate the potential for sensitivity enhancement by considering a CPW structure, the step-impedance design line consists of a single 90º line section. For sensitivity optimization, such line section must exhibit high characteristic impedance, following the indications of the previous section (and reported in [21]). Particularly, the impedance of such line section is set to Z_1 = 70 Ω. By considering the implementation on the *Rogers RO3010* substrate with thickness h = 1.27 mm and dielectric constant ε_r = 10.2, the resulting topology of the sensor is the one shown in Fig. 3(a), where the relevant dimensions are indicated (note that the sensor is completed with a 50Ω access line).

For sensor B, the electrical length and characteristic impedance of the open-ended sensing line are set to 90º and Z_s = 70 Ω, respectively (i.e., a high impedance line, as required for such phase). Therefore, in this case, the (single section) 90º design line must exhibit a low impedance value (specifically, Z_1 = 35 Ω). By considering identical substrate and operating frequency as those for sensor A, the layout of sensor B is the one depicted in Fig. 3(b).

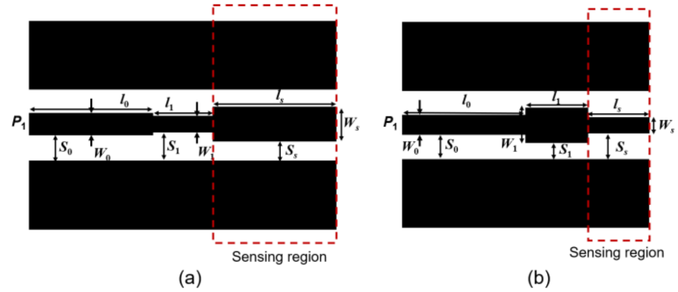

Fig. 3. Layout of the designed reflective-mode CPW phase-variation sensors. (a) Sensor A; (b) sensor B. For sensor A, dimensions are: W_s = 2.26 mm, S_s = 0.27 mm, l_s = 32.25 mm (180º), W_1 = 0.72 mm, S_1 = 1.04 mm, l_1 = 16.32 mm (90º), W_0 = 1.38 mm, S_0 = 0.71 mm, l_0 = 32.95 mm (180º); for sensor B, the dimensions of the sensing line are those for the design line in sensor A, whereas the dimensions of the design line are those for the sensing line in sensor A, with the exception of the length l_1 = 16.56 mm (90º) and l_s = 15.46 mm. The sensing regions are indicated by dashed rectangles.

Before fabrication, we have inferred the phase of the reflection coefficient for sensors A and B, by considering the sensing lines loaded with semi-infinite (in the vertical direction) MUTs of varying dielectric constant (Fig. 4). In this case, the electromagnetic simulation has been carried out by means of the *CST Microwave Studio* commercial simulator, since the dimensions of the samples are finite in both horizontal directions.

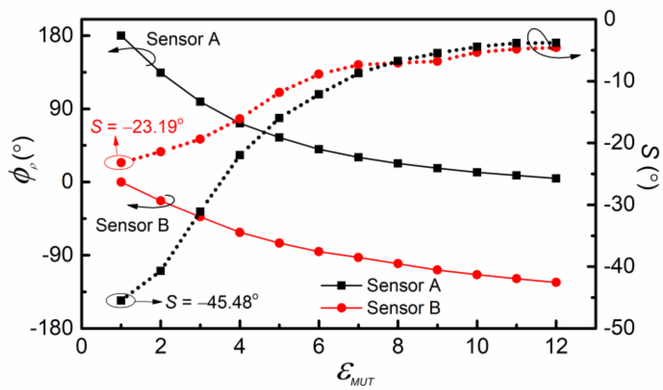

Fig. 4. Simulated phase of the reflection coefficient for sensors A and B by considering MUTs with different dielectric constant, and sensitivity.

In the limit of small perturbations (low value of the ε_{MUT}, or $\varepsilon_{MUT} \rightarrow 1$), the sensitivity is calculated according to (1), using (5) and $S_{\phi_s} = d\phi_\rho/d\phi_s$ given by [21]

$$S_{\phi_s} = \frac{d\phi_\rho}{d\phi_s} = -\frac{2Z_1^2}{Z_0 Z_s} \tag{8}$$

for sensor A, and by

$$S_{\phi_s} = \frac{d\phi_\rho}{d\phi_s} = -\frac{2Z_0 Z_s}{Z_1^2} \tag{9}$$

for sensor B. Note that (8) and (9) contribute significantly to sensitivity enhancement. The reason is that for (8), corresponding to sensor A, the impedances satisfy $Z_1 > Z_0 > Z_s$, whereas for sensor B the impedances have been chosen according to $Z_1 < Z_0 < Z_s$ (thereby providing significant values for (8) and (9)). With the considered values of the impedances (given before) and $Z_0 = 50\ \Omega$ (reference impedance of the ports), evaluation of (8) and (9) provides $S_{\phi s} = -5.60$ for sensor A and $S_{\phi s} = -5.71$ for sensor B, respectively. On the other hand, evaluation of (5) in the limit of small perturbations gives $d\phi_s/d\varepsilon_{MUT} = 8.18^o$ and $d\phi_s/d\varepsilon_{MUT} = 3.92^o$ for sensors A and B, respectively. Consequently, the total sensitivity for small perturbations (1) is found to be $S = -45.81^o$ and $S = -22.38^o$ for sensors A and B, respectively. The sensitivities inferred from the simulated data of Fig. 4 are also depicted in that figure. It can be appreciated, that the sensitivity is a maximum for small perturbations and it coincides with the analytical results to a very good approximation (the values of the simulations are $S = -45.48^o$ and $S = -23.19^o$ for sensors A and B, respectively).

It should be emphasized that (8) and (9) are valid for sensing line electrical lengths of 180º and 90º, respectively. Since for the considered sensors, the corresponding sensing lines satisfy this phase requirement when they are uncovered, the sensitivity values calculated through (1) and (8) or (9), are valid in the limit when $\varepsilon_{MUT} \rightarrow 1$. Nevertheless, sensitivity can be optimized for other values of ε_{MUT} (the reference dielectric constant) by simply recalculating the length of the sensing line so that its phase is either 180º or 90º when it is covered by the material with the reference dielectric constant.

IV. Experimental validation

For experimental validation, the CPW sensors designed in the previous section have been fabricated by means of a *LPKF H100* drilling machine. Moreover, for comparison purposes, we have also fabricated a step-impedance phase-variation sensor implemented in microstrip technology, using identical substrate. In particular, the microstrip based sensor is composed of an open-ended 90º sensing line with characteristic impedance $Z_s = 70\ \Omega$, cascaded to a design line with $\phi = 90^o$ and $Z_1 = 35\ \Omega$, that is, equivalent to the CPW sensor B. The photographs of the three fabricated sensors are depicted in Fig. 5 (the dimensions of the microstrip-based sensor are given in the caption).

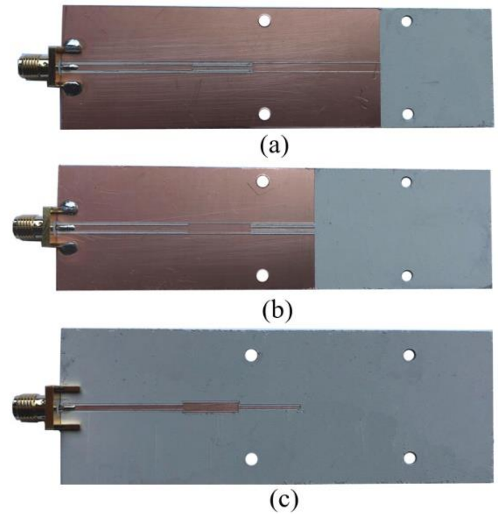

Fig. 5. Photograph of the fabricated sensors. (a) CPW sensor A; (b) CPW sensor B; (c) microstrip sensor. For the microstrip sensor, dimensions are: $W_s = 0.46$ mm, $l_s = 14.36$ mm (90º), $W_1 = 2.12$ mm, $l_1 = 12.69$ mm (90º), $W_0 = 1.00$ mm, $l_0 = 27.30$ mm (180º).

The three sensors have been loaded with identical MUT samples, consisting of different uncladded microwave substrates with similar thickness (i.e., around 3 mm, corresponding to two pieces of slabs stacked up together) and well-known dielectric constant. With such MUT thickness, the semi-infinite MUT approximation (particularly (5) and (6)) is reasonably valid. Therefore, the maximum sensitivity (the one for small perturbations) can be predicted by the theory to a good approximation for these particular MUT thicknesses. Nevertheless, an effective comparison between the different sensors can be made regardless of the validity of the semi-infinite MUT approximation, as far as identical MUTs are used in all cases. Indeed, the main conclusions relative to the enhanced sensitivity by using a CPW structure, rather than a step-impedance microstrip line, are valid regardless of the thickness of the MUT.

Figure 6 depicts the measured phase of the reflection coefficient for the different MUTs (indicated in the caption), relative to the phase of the bare sensor. As it can be seen, the phase of the reflection coefficient experiences a stronger variation with the dielectric constant for the CPW sensor based on the 180º sensing line (sensor A), in accordance with the simulations of Section III (based on a semi-infinite MUT). Note that the sensitivity is superior to the one of sensor B. The main reason is the longer sensing line considered in sensor A, as compared to sensor B (roughly twice). The microstrip based sensor, equivalent to sensor B, exhibits smaller sensitivity than the CPW counterpart, thereby confirming the enhanced sensitivity achievable by implementing the sensors in CPW technology. Figure 6 also includes the simulated phase of Fig. 4 for sensors A and B, in reference to the phase of the bare sensor, as well as the simulated phase of the microstrip sensor. The agreement is reasonably good, thereby pointing out the validity of the semi-infinite MUT approximation. The higher discrepancy that appears for the PLA slab is attributed to the fact that such sample has been 3D-printed, and probably the dielectric constant of such material, as inferred from independent measurements using a resonant cavity, has been overestimated.

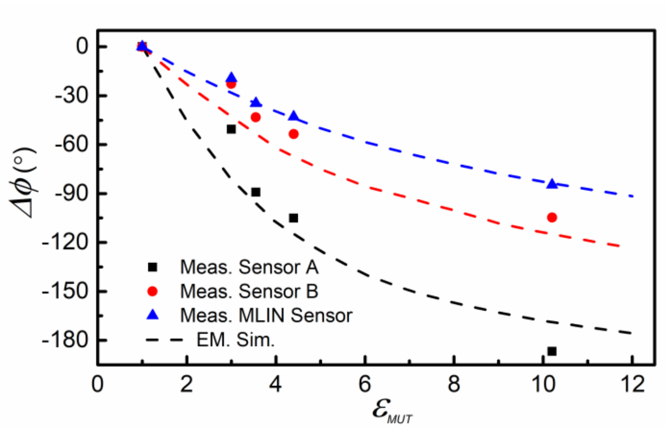

Fig. 6. Measured phase of the reflection coefficient relative to the phase of the bare sensor, i.e., $\Delta\phi = \phi_\rho - \phi_{\rho,\text{air}}$, as a function of the dielectric constant of the MUT sample. The considered MUTs are: air ($\varepsilon_{MUT} = 1$), PLA ($\varepsilon_{MUT} = 3$), *Rogers 4003C* ($\varepsilon_{MUT} = 3.5$), *FR4* ($\varepsilon_{MUT} = 4.5$), and *Rogers 3010* ($\varepsilon_{MUT} = 10.2$).

It is remarkable that these sensors exhibit very competitive sensitivity by virtue of the step-impedance discontinuity, as discussed in [21]. This sensitivity is further enhanced by implementing the sensors in CPW technology, as far as these lines exhibit a stronger variation of the phase velocity (and hence electrical length) with the dielectric constant of the MUT. This is an important aspect to maximize the term $d\phi_s/d\varepsilon_{MUT}$ of the right-hand side member in (1), thereby optimizing the overall sensor sensitivity without the need to excessively enhance the first term, i.e., S_{ϕ_s}. According to (8) and (9), such term increases with the impedance contrast, and it can be further enhanced by cascading additional 90º line sections with alternate high and low impedance [21]. Thus, with CPW structures, high sensitivity can be obtained by relaxing the requirements of high impedance contrasts and an excessive number of line sections for the step-impedance design line. This has direct impact on sensor size and sensor implementation (i.e., excessive high or low line impedances may not be implementable).

Besides the maximum sensitivity (–45.48º and –23.19º for sensors A and B, respectively), other important sensor parameters are the output dynamic range, related to the average sensitivity, and sensor resolution. By considering an input dynamic range for the dielectric constant of [1-10.2], the output dynamic ranges for sensors A and B are found to be 165º and, 105º, respectively). By considering that phase variations of 5º can be discriminated (a very conservative value), the dielectric constant resolution in the limit of small perturbations is 0.11 for sensor A and 0.21 for sensor B.

The reported sensors are especially suited in applications where high sensitivity to small variations of dielectric constant are required. This includes analysis of material composition, liquid mixtures, solute concentration measurements, and defect detection, among others. In all these cases, changes in material composition, solute concentration, or the presence of defects in the MUT can be inferred from the variation experienced by the dielectric constant (or effective dielectric constant) of the MUT. To illustrate the potential of the proposed sensors to detect tiny defects in samples, we have drilled holes in a specific substrate (*Rogers RO3010* with 1.27 mm thickness of Fig. 6). The holes are arranged in sparse square grids, and several samples, with different hole densities, have been prepared (the pictures are depicted in Fig. 7). We have measured the phase of the reflection coefficient for the different samples, in reference to the one of the sample without holes, by using sensor A. However, the design has been slightly modified in order to obtain a 180º sensing line when it is loaded with the reference substrate (i.e., without holes). This optimizes the sensitivity, as far as the presence of holes in the MUT generates small perturbations in the vicinity of the nominal value of the phase of the sensing line (180º for sensor A), as required for sensitivity optimization. The new geometrical variables for the sensing line are found to be $l_s = 24.00$ mm, $W_s = 2.26$ mm, and $S_s = 0.27$ mm. The results, depicted in Fig. 8, demonstrate the potential of the sensor to discern and detect the presence of defects, even for the MUT sample with the smaller density of holes.

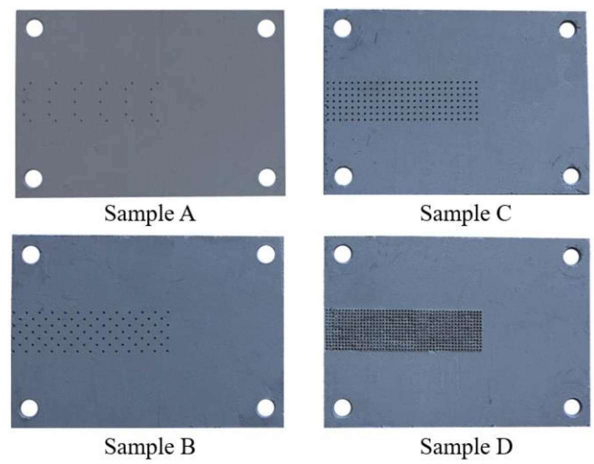

Fig. 7. Photographs of the MUT samples with drilled hole arrays.

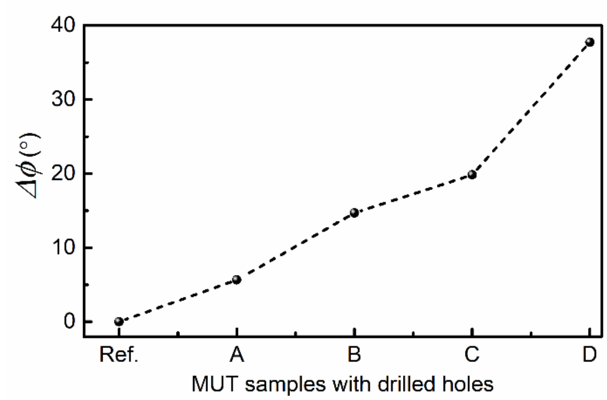

Fig. 8. Measured phase of the reflection coefficient for sensor A (slightly modified as mentioned in the text) for different MUT samples with drilled holes, relative to the phase of the sensor loaded with the MUT without holes (reference sample of *Rogers RO3010* without holes).

V. Comparison to Other Similar Sensors

As mentioned before, the main advantage of the proposed CPW based sensors over the microstrip counterparts is the fact that the sensitivity can be improved due to the higher dependence of the phase (or electrical length) of the sensing line with the dielectric constant of the MUT (this is explained because the electric field lines generated in the sensing line penetrate more into the MUT under consideration for the CPW based sensor). Nevertheless, the reported maximum sensitivities in [21] are superior (528.7º) due to the different considered conditions (i.e., number of step-impedance stages, dielectric constant of the sensor substrate, considered impedance contrasts, etc.). The phase-variation CPW and microstrip based sensors reported in this paper and those reported in [21] operate in reflection mode. Other phase-variation sensors operating in transmission have been recently reported [17],[18]. In [18], the sensitivity is very high (415.6º), but at the expense of a relatively high operating frequency (6 GHz) and dimensions of the sensing area (105.6 cm^2). In [17], the dimensions of the sensitive part of the sensor are smaller, but the operating frequency is 10 GHz for a sensitivity (54.85º) comparable to the one of sensor A of this paper.

It should be also mentioned that in other transmission-mode phase-variation sensors reported in the literature, the phase information is converted to magnitude information, thereby making the comparison difficult. Nevertheless, let us highlight the good sensitivity achieved in the sensors reported in [40] and [48], i.e., 600 dB and 25.3 dB, respectively, by virtue of the controllable dispersion of the considered sensing lines, implemented by means of a composite right/left handed line in [40], and by means of an electro-inductive wave transmission line in [48]. However, the dimensions of the sensitive region of these sensors are, in general, large as compared to the dimensions of the sensors reported in this paper (note that the sensing region is either a 90º or a 180º sensing line). Moreover, in the sensors reported in [40],[48], once the sensing line is designed, further increasing the sensitivity necessarily requires elongating such line. By contrast, in the sensors of this paper, sensitivity enhancement can be carried out by merely adding step-impedance stages, keeping the dimensions of the sensing line unaltered. Let us also mention that in [49], a phase-variation transmission-mode differential sensor with good sensitivity (17.6 dB) was reported. In such sensor the phase information was transformed to magnitude information by means of a pair of rat-race hybrid couplers. This increases the overall size of the sensors, as also occurs in the implementation of [40].

In summary, the combination of performance and dimensions of the sensors reported in this paper is very competitive. Moreover, sensor design and implementation is extremely easy, as far as these sensors consist of a simple open-ended step-impedance transmission line configuration. Finally, the proposed sensors are also useful for measuring variables related to the dielectric constant, for example defect detection, as discussed before, and characterization of the solute content in liquid solutions, as far as the solute content determines the dielectric constant of the liquid mixture (in this case, fluidic channels in the sensing structure should be introduced [45],[46],[51],[53],[54]).

VI. Conclusions

In conclusion, it has been demonstrated in this paper that the sensitivity of reflective-mode phase-variation sensors based on step-impedance transmission lines can be optimized by implementing the sensor in CPW technology. Analytical expressions providing the sensitivity have been obtained and validated by full-wave electromagnetic simulation. Finally, the potential of the CPW sensors for sensitivity improvement as compared to their microstrip counterparts has been verified experimentally by measuring the phase of the reflection coefficient in both CPW and microstrip-based sensors loaded with different MUT samples. The ability of the sensors to detect the presence of tiny defects in MUT samples (emulated in this work by drilling holes in a commercial microwave substrate), has been also demonstrated. These sensors are fully planar, do not include vias or defected ground structures, operate at a single frequency, and work in reflective mode. All these characteristics, plus the highly achievable sensitivity, are key aspects for the future application of the reported structures in real scenarios.

References

[1] M. Puentes, C. Weiß, M. Schüßler, and R. Jakoby, “Sensor array based on split ring resonators for analysis of organic tissues,” in *IEEE MTT-S Int. Microw. Symp.*, Baltimore, MD, USA, Jun. 2011, pp. 1−4.

[2] A. Ebrahimi, W. Withayachumnankul, S. Al-Sarawi, and D. Abbott, “High-sensitivity metamaterial-inspired sensor for microfluidic dielectric characterization,” *IEEE Sens. J.*, vol. 14, no. 5, pp. 1345−1351, May 2014.

[3] M. Schüßler, C. Mandel, M. Puentes, and R. Jakoby, “Metamaterial inspired microwave sensors,” *IEEE Microw. Mag.*, vol. 13, no. 2, pp. 57–68, Mar. 2012.

[4] M. S. Boybay and O. M. Ramahi, “Material characterization using complementary split-ring resonators,” *IEEE Trans. Instrum. Meas.*, vol. 61, no. 11, pp. 3039−3046, Nov. 2012.

[5] C.-S. Lee and C.-L. Yang, “Complementary split-ring resonators for measuring dielectric constants and loss tangents,” *IEEE Microw. Wireless Compon. Lett.*, vol. 24, no. 8, pp. 563−565, Aug. 2014.

[6] C.-L. Yang, C.-S. Lee, K.-W. Chen, and K.-Z. Chen, “Noncontact measurement of complex permittivity and thickness by using planar resonators,” *IEEE Trans. Microw. Theory Techn.*, vol. 64, no.1, pp. 247−257, Jan. 2016.

[7] L. Su, J. Mata-Contreras, P. Vélez, and F. Martín, “Estimation of the complex permittivity of liquids by means of complementary split ring resonator (CSRR) loaded transmission lines,” in *2017 IEEE MTT-S International Microwave Workshop Series on Advanced Materials and Processes* (IMWS-AMP 2017), Pavia, Italy, 20-22 Sep. 2017.

[8] L. Su, J. Mata-Contreras, P. Vélez, A. Fernández-Prieto, and F. Martín, “Analytical method to estimate the complex permittivity of oil samples,” *Sensors*, 18(4), paper 984, 2018.

[9] A.K. Jha, N. Delmonte, A. Lamecki, M. Mrozowski, and M. Bozzi, “Design of microwave-based angular displacement sensor,” *IEEE Microw. Wireless Compon. Lett.*, vol. 29 (4), pp. 306−308, Apr. 2019.

[10] G. Galindo-Romera, F. Javier Herraiz-Martínez, M. Gil, J. J. Martínez-Martínez, and D. Segovia-Vargas, “Submersible printed split-ring resonator-based sensor for thin-film detection and permittivity characterization,” *IEEE Sens. J.*, vol. 16, no. 10, pp. 3587−3596, May 2016.

[11] R. A. Alahnomi, Z. Zakaria, E. Ruslan, S. R. A. Rashid, and A. A. M. Bahar, “High-Q sensor based on symmetrical split ring resonator with spurlines for solids material detection,” *IEEE Sens. J.*, vol. 17, no. 9, pp. 2766−2775, May 2017.

[12] N. Jankovic and V. Radonic, “A microwave microfluidic sensor based on a dual-mode resonator for dual-sensing applications,” *Sensors*, vol. 17(12), p. 2713, 2017.

[13] H. Zhou, D. Hu, C. Yang, C. Chen, J. Ji, M. Chen, Y. Chen, Y. Yang, and X. Mu, “Multi-band sensing for dielectric property of chemicals using metamaterial integrated microfluidic sensor,” *Sci. Rep.*, vol. 8(1), pp. 1−11, Oct. 2018.

[14] M. A. H. Ansari, A. K. Jha, Z. Akhter, and M. J. Akhtar, “Multi-band RF planar sensor using complementary split ring resonator for testing of dielectric materials,” *IEEE Sens. J.*, vol. 18, no. 16, pp. 6596−6606, Aug. 2018.

[15] H. Lobato-Morales, J. H. Choi, H. Lee, and J. L. Medina-Monroy, "Compact dielectric-permittivity sensors of liquid samples based on substrate-integrated-waveguide with negative-order-resonance," *IEEE Sens. J*., vol. 19, no. 19, pp. 8694−8699, Oct. 2019.

[16] Y. Khanna and Y.K Awasthi, "Dual-band microwave sensor for investigation of liquid impurity concentration using a metamaterial complementary split-ring resonator," *J. Elect. Mat*., vol 49, pp. 385–394, 2020.

[17] F.J. Ferrández-Pastor, J.M. García-Chamizo, and M. Nieto-Hidalgo, "Electromagnetic differential measuring method: application in microstrip sensors developing," *Sensors*, vol. 17, p. 1650, 2017.

[18] J. Muñoz-Enano, P. Vélez, M. Gil, and F. Martín, "An analytical method to implement high sensitivity transmission line differential sensors for dielectric constant measurements," *IEEE Sens. J.*, vol. 20, pp. 178–184, Jan. 2020.

[19] A. K. Jha, A. Lamecki, M. Mrozowski, and M. Bozzi, "A highly sensitive planar microwave sensor for detecting direction and angle of rotation," *IEEE Trans. Microw. Theory Techn*., vol. 68, no. 4, pp. 1598–1609, Apr. 2020.

[20] A. K. Horestani, Z. Shaterian, and F. Martín, "Rotation sensor based on the cross-polarized excitation of split ring resonators (SRRs)," *IEEE Sens. J*., vol. 20, no. 17, pp. 9706–9714, Apr. 2020.

[21] J. Muñoz-Enano, P. Vélez, L. Su, M. Gil, P. Casacuberta, and F. Martín, "On the sensitivity of reflective-mode phase-variation sensors based on open-ended stepped-impedance transmission lines: theoretical analysis and experimental validation," *IEEE Trans. Microw. Theory Techn*., to be published.

[22] A. K. Horestani, J. Naqui, Z. Shaterian, D. Abbott, C. Fumeaux, and F. Martín, "Two-dimensional alignment and displacement sensor based on movable broadside-coupled split ring resonators," *Sensors and Actuators A*, vol. 210, pp. 18–24, Apr. 2014.

[23] J. Naqui, C. Damm, A. Wiens, R. Jakoby, L. Su, and F. Martín, "Transmission lines loaded with pairs of magnetically coupled stepped impedance resonators (SIRs): modeling and application to microwave sensors," in *IEEE MTT-S Int. Microwave Symp*., Tampa, FL, USA, Jun. 2014, pp. 1–4.

[24] L. Su, J. Naqui, J. Mata-Contreras, and F. Martín, "Modeling metamaterial transmission lines loaded with pairs of coupled split ring resonators," *IEEE Ant. Wireless Propag. Lett.*, vol. 14, pp. 68–71, 2015.

[25] L. Su, J. Naqui, J. Mata-Contreras, and F. Martín, "Modeling and applications of metamaterial transmission lines loaded with pairs of coupled complementary split ring resonators (CSRRs)," *IEEE Ant. Wireless Propag. Lett.*, vol. 15, pp. 154–157, 2016.

[26] L. Su, J. Mata-Contreras, J. Naqui, and F. Martín, "Splitter/combiner microstrip sections loaded with pairs of complementary split ring resonators (CSRRs): modeling and optimization for differential sensing applications," *IEEE Trans. Microw. Theory Techn*., vol. 64, pp. 4362–4370, Dec. 2016.

[27] A. Ebrahimi, J. Scott, and K. Ghorbani, "Differential sensors using microstrip lines loaded with two split ring resonators," *IEEE Sens. J.*, vol. 18, pp. 5786–5793, Jul. 2018.

[28] P. Vélez, L. Su, K. Grenier, J. Mata-Contreras, D. Dubuc, and F. Martín, "Microwave microfluidic sensor based on a microstrip splitter/combiner configuration and split ring resonators (SRR) for dielectric characterization of liquids," *IEEE Sens. J.*, vol. 17, pp. 6589–6598, Oct. 2017.

[29] J. Naqui, M. Durán-Sindreu, and F. Martín, "Novel sensors based on the symmetry properties of split ring resonators (SRRs)," *Sensors*, vol. 11, pp. 7545−7553, 2011.

[30] J. Naqui, M. Durán-Sindreu, and F. Martín, "Alignment and position sensors based on split ring resonators," *Sensors*, vol. 12, pp. 11790−11797, 2012.

[31] A.K. Horestani, C. Fumeaux, S.F. Al-Sarawi, and D. Abbott, "Displacement sensor based on diamond-shaped tapered split ring resonator," *IEEE Sens. J*., vol. 13, pp. 1153–1160, 2013.

[32] A.K. Horestani, D. Abbott, and C. Fumeaux, "Rotation sensor based on horn-shaped split ring resonator," *IEEE Sens. J.*, vol. 13, pp. 3014–3015, 2013.

[33] J. Naqui and F. Martín, "Transmission lines loaded with bisymmetric resonators and their application to angular displacement and velocity sensors," *IEEE Trans. Microw. Theory Techn.*, vol. 61, no. 12, pp. 4700–4713, Dec. 2013.

[34] J. Naqui and F. Martín, "Angular displacement and velocity sensors based on electric-LC (ELC) loaded microstrip lines," *IEEE Sens. J.*, vol. 14, no. 4, pp. 939–940, Apr. 2014.

[35] A.K. Horestani, J. Naqui, D. Abbott, C. Fumeaux, and F. Martín, "Two-dimensional displacement and alignment sensor based on reflection coefficients of open microstrip lines loaded with split ring resonators," *Elec. Lett.*, vol. 50, pp. 620–622, Apr. 2014.

[36] A. Ebrahimi, W. Withayachumnankul, S. F. Al-Sarawi, and D. Abbott, "Metamaterial-inspired rotation sensor with wide dynamic range," *IEEE Sens. J*., vol. 14, no. 8, pp. 2609–2614, Aug. 2014.

[37] J. Naqui, J. Coromina, A. Karami-Horestani, C. Fumeaux, and F. Martín, "Angular displacement and velocity sensors based on coplanar waveguides (CPWs) loaded with S-shaped split ring resonator (S-SRR)," *Sensors*, vol. 15, pp. 9628–9650, 2015.

[38] J. Mata-Contreras, C. Herrojo, and F. Martín, "Application of split ring resonator (SRR) loaded transmission lines to the design of angular displacement and velocity sensors for space applications," *IEEE Trans. Microw. Theory Techn*., vol. 65, no. 11, pp. 4450–4460, Nov. 2017.

[39] J. Mata-Contreras, C. Herrojo, and F. Martín, "Detecting the rotation direction in contactless angular velocity sensors implemented with rotors loaded with multiple chains of split ring resonators (SRRs)," *IEEE Sens. J*., vol.18, no. 17, pp. 7055–7065, Sep. 2018.

[40] C. Damm, M. Schussler, M. Puentes, H. Maune, M. Maasch, and R. Jakoby, "Artificial transmission lines for high sensitive microwave sensors," in *IEEE Sensors Conf.*, Christchurch, New Zealand, pp.755−758, Oct. 2009.

[41] J. Muñoz-Enano, P. Vélez, M. Gil, and F. Martín, "Planar microwave resonant sensors: a review and recent developments," *Appl. Sci*., vol. 10, no. 7, p. 2615, Jan. 2020.

[42] P. Vélez, J. Mata-Contreras, L. Su, D. Dubuc, K. Grenier, and F. Martín, "Modeling and analysis of pairs of open complementary split ring resonators (OCSRRs) for differential permittivity sensing," in *2017 IEEE MTT-S International Microwave Workshop Series on Advanced Materials and Processes* (IMWS-AMP 2017), Pavia, Italy, 20-22 Sept. 2017.

[43] P. Vélez, K. Grenier, J. Mata-Contreras, D. Dubuc, and F. Martín, "Highly-sensitive microwave sensors based on open complementary split ring resonators (OCSRRs) for dielectric characterization and solute concentration measurement in liquids," *IEEE Access*, vol. 6, pp. 48324–48338, Aug. 2018.

[44] A. Ebrahimi, J. Scott, and K. Ghorbani, "Transmission lines terminated with LC resonators for differential permittivity sensing," *IEEE Microw. Wireless Compon. Lett*., vol. 28, no. 12, pp. 1149–1151, Dec. 2018.

[45] P. Vélez, J. Muñoz-Enano, K. Grenier, J. Mata-Contreras, D. Dubuc, and F. Martín, "Split ring resonator (SRR) based microwave fluidic sensor for electrolyte concentration measurements," *IEEE Sens. J.*, vol. 19, no. 7, pp. 2562–2569, Apr. 2019.

[46] P. Vélez, J. Muñoz-Enano, M. Gil, J. Mata-Contreras, and F. Martín, "Differential microfluidic sensors based on dumbbell-shaped defect ground structures in microstrip technology: analysis, optimization, and applications," *Sensors*, vol. 19, p. 3189, 2019.

[47] P. Vélez, J. Muñoz-Enano, and F. Martín, "Differential sensing based on quasi-microstrip-mode to slot-mode conversion," *IEEE Microw. Wireless Compon. Lett*., vol. 29, pp. 690–692, Oct. 2019.

[48] M. Gil, P. Vélez, F. Aznar-Ballesta, J. Muñoz-Enano, and F. Martín, "Differential sensor based on electro-inductive wave (EIW) transmission lines for dielectric constant measurements and defect detection," *IEEE Trans. Ant. Propag*., vol. 68, no. 3, pp. 1876–1886, Mar. 2020.

[49] J. Muñoz-Enano, P. Vélez, M. Gil, J. Mata-Contreras, and F. Martín, "Differential-mode to common-mode conversion detector based on rat-race couplers: analysis and application to microwave sensors and comparators," *IEEE Trans. Microw. Theory Techn*., vol. 68, pp. 1312–1325, Apr. 2020.

[50] A. Ebrahimi, J. Scott, and K. Ghorbani, "Microwave reflective biosensor for glucose level detection in aqueous solutions," *Sens. & Act. A: Physical*, vol. 301, p. 111662, 2020.

[51] J. Muñoz-Enano, P. Vélez, M. Gil, and F. Martín, "Microfluidic reflective-mode differential sensor based on open split ring resonators (OSRRs)," *Int. J. Microw. Wireless Technol*., 2020, published online.

[52] D.M. Pozar, *Microwave Engineering*, 4th Ed., John Wiley, Hoboken, NJ, 2011.

[53] A. Ebrahimi, J. Scott, and K. Ghorbani, "Ultrahigh-sensitivity microwave sensor for microfluidic complex permittivity measurement," *IEEE Trans. Microw. Theory Techn*., vol. 67, no. 10, pp. 4269–4277, Oct. 2019.

[54] A. Ebrahimi, F. J. Tovar-Lopez, J. Scott, and K. Ghorbani, "Differential microwave sensor for characterization of glycerol–water solutions," *Sens. & Act. B: Chem.*, vol. 321, Art. no. 128561, 2020.

Lijuan Su was born in Qianjiang (Hubei), China in 1983. She received the B.S. degree in communication engineering and the M.S. degree in circuits and systems both from Wuhan University of Technology, Wuhan, China, in 2005 and 2013 respectively, and the Ph.D. degree in electronic engineering from Universitat Autonoma de Barcelona, Barcelona, Spain, in 2017. From Nov. 2017 to Dec. 2019, she worked as a postdoc researcher in Flexible Electronics Research Center, Huazhong University of Science and Technology, Wuhan, China. She is currently a postdoc researcher in CIMITEC, Universitat Autonoma de Barcelona, Spain. Her current research interests focus on the development of novel microwave sensors with improved performance for biosensors, dielectric characterization of solids and liquids, defect detection, industrial processes, etc.

Jonathan Muñoz-Enano was born in Mollet del Vallès (Barcelona), Spain, in 1994. He received the Bachelor's Degree in Electronic Telecommunications Engineering in 2016 and the Master's Degree in Telecommunications Engineering in 2018, both at the Autonomous University of Barcelona (UAB). Actually, he is working in the same university in the elaboration of his PhD, which is focused on the development of microwave sensors based on metamaterials concepts for the dielectric characterization of materials and biosensors.

Paris Vélez (S'10–M'14) was born in Barcelona, Spain, in 1982. He received the degree in Telecommunications Engineering, specializing in electronics, the Electronics Engineering degree, and the Ph.D. degree in Electrical Engineering from the Universitat Autònoma de Barcelona, Barcelona, in 2008, 2010, and 2014, respectively. His Ph.D. thesis concerned common mode suppression differential microwave circuits based on metamaterial concepts and semi-lumped resonators. During the Ph.D., he was awarded with a pre-doctoral teaching and research fellowship by the Spanish Government from 2011 to 2014. From 2015-2017, he was involved in the subjects related to metamaterials sensors for fluidics detection and characterization at LAAS-CNRS through a TECNIOSpring fellowship cofounded by the Marie Curie program. His current research interests include the miniaturization of passive circuits RF/microwave and sensors-based metamaterials through Juan de la Cierva fellowship. Dr. Vélez is a Reviewer for the IEEE Transactions on Microwave Theory and Techniques and for other journals.

Pau Casacuberta was born in Sabadell (Barcelona), Spain, in 1997. Currently, he is in his senior year of the Bachelor's Degree in Electronic Telecommunications Engineering and the Bachelor's Degree in Computer Engineering, both at the Universitat Autònoma de Barcelona (UAB). He received the Collaboration fellowship by the Spanish Government in 2019 for developing his Bachelor's Thesis in highly sensitive reflective-mode microwave sensors based on stepped-impedance transmission lines.

Marta Gil (S'05-M'09) was born in Valdepeñas, Ciudad Real, Spain, in 1981. She received the Physics degree from Universidad de Granada, Spain, in 2005, and the Ph.D. degree in electronic engineering from the Universitat Autònoma de Barcelona, Barcelona, Spain, in 2009. She studied one year with the Friedrich Schiller Universität Jena, Jena, Germany. During her PhD Thesis she was holder of a METAMORPHOSE NoE grant and National Research Fellowship from the FPU Program of the Education and Science Spanish Ministry. As a postdoctoral researcher, she was awarded with a Juan de la Cierva fellowship working in the Universidad de Castilla-La Mancha. She was postdoctoral researcher in the Institut für Mikrowellentechnik und Photonik in Technische Universität Darmstadt and in the Carlos III University of Madrid. She is currently assistant professor in the Universidad Politécnica de Madrid. She has worked in metamaterials, piezoelectric MEMS and microwave passive devices. Her current interests include metamaterials sensors for fluidic detection.

Ferran Martín (M'04-SM'08-F'12) was born in Barakaldo (Vizcaya), Spain in 1965. He received the B.S. Degree in Physics from the Universitat Autònoma de Barcelona (UAB) in 1988 and the PhD degree in 1992. From 1994 up to 2006 he was Associate Professor in Electronics at the Departament d'Enginyeria Electrònica (Universitat Autònoma de Barcelona), and since 2007 he is Full Professor of Electronics. In recent years, he has been involved in different research activities including modelling and simulation of electron devices for high frequency applications, millimeter wave and THz generation systems, and the application of electromagnetic bandgaps to microwave and millimeter wave circuits. He is now very active in the field of metamaterials and their application to the miniaturization and optimization of microwave circuits and antennas. Other topics of interest include microwave sensors and RFID systems, with special emphasis on the development of high data capacity chipless-RFID tags. He is the head of the Microwave Engineering, Metamaterials and Antennas Group (GEMMA Group) at UAB, and director of CIMITEC, a research Center on Metamaterials supported by TECNIO (Generalitat de Catalunya). He has organized several international events related to metamaterials and related topics, including Workshops at the IEEE International Microwave Symposium (years 2005 and 2007) and European Microwave Conference (2009, 2015 and 2017), and the Fifth International Congress on Advanced Electromagnetic Materials in Microwaves and Optics (Metamaterials 2011), where he acted as Chair of the Local Organizing Committee. He has acted as Guest Editor for six Special Issues on metamaterials and sensors in five International Journals. He has authored and co-authored over 600 technical conference, letter, journal papers and book chapters, he is co-author of the book on Metamaterials entitled Metamaterials with Negative Parameters: Theory, Design and Microwave Applications (John Wiley & Sons Inc.), author of the book Artificial Transmission Lines for RF and Microwave Applications (John Wiley & Sons Inc.), co-editor of the book Balanced Microwave Filters (Wiley/IEEE Press) and co-author of the book Time-Domain Signature Barcodes for Chipless-RFID and Sensing Applications (Springer). Ferran Martín has generated 21 PhDs, has filed several patents on metamaterials and has headed several Development Contracts.

Prof. Martín is a member of the IEEE Microwave Theory and Techniques Society (IEEE MTT-S). He is reviewer of the IEEE Transactions on Microwave Theory and Techniques and IEEE Microwave and Wireless Components Letters, among many other journals, and he serves as member of the Editorial Board of IET Microwaves, Antennas and Propagation, International Journal of RF and Microwave Computer-Aided Engineering, and Sensors. He is also a member of the Technical Committees of the European Microwave Conference (EuMC) and International Congress on Advanced Electromagnetic Materials in Microwaves and Optics (Metamaterials). Among his distinctions, Ferran Martín has received the 2006 Duran Farell Prize for Technological Research, he holds the Parc de Recerca UAB – Santander Technology Transfer Chair, and he has been the recipient of three ICREA ACADEMIA Awards (calls 2008, 2013 and 2018). He is Fellow of the IEEE and Fellow of the IET.